

# mAPm: multi-scale Attention Pyramid module for Enhanced scale-variation in RLD detection.

Haruna Yunusa<sup>1</sup>, Qin Shiyin<sup>1</sup>, Abdulrahman Hamman Adama Chukkol<sup>2</sup>, Isah Bello<sup>3</sup>,  
and Adamu Lawan<sup>1</sup>

<sup>1</sup> Beihang University, <sup>2</sup> Beijing Institute of Technology, <sup>3</sup> Tianjin University, China

**Abstract.** Detecting objects across various scales remains a significant challenge in computer vision, particularly in tasks such as Rice Leaf Disease (RLD) detection where objects exhibit considerable scale variations. Traditional object detection methods often struggle to address these variations, resulting in missed detections or reduced accuracy. In this study, we propose the multi-scale Attention Pyramid module (mAPm), a novel approach that integrates dilated convolutions into the Feature Pyramid Network (FPN) to enhance multi-scale information extraction. Additionally, we incorporate a global Multi-Head Self-Attention (MHSA) mechanism and a deconvolutional layer to refine the up-sampling process. We evaluate mAPm on YOLOv7 using the MRLD and COCO datasets. Compared to vanilla FPN, BiFPN, NAS-FPN, PANET, and ACFPN, mAPm achieved a significant improvement in Average Precision (AP), with a +2.61% increase on the MRLD dataset compared to the baseline FPN method in YOLOv7. This demonstrates its effectiveness in handling scale variations. Furthermore, the versatility of mAPm allows its integration into various FPN-based object detection models, showcasing its potential to advance object detection techniques.

**Keywords:** Attention Mechanism, Feature Pyramid Network, Object Detection, Scale-variation.

## 1 Introduction

In spite of the successes of object detection in computer vision (CV), it still faces some real challenges with respect to task objectives and constraints. One such problem is scale variation because object detectors are required to detect objects at different scales [1]. Scale variation can either be the change of object size or box aspect ratio. For example, objects are viewed in a camera from varying distances which results in a variation of an object bounding box, while some objects can be very flat or thin (leaves, knives, forks, chopsticks, etc.). In essence, objects appear with arbitrary sizes ranging from the entire image to a few pixels. The extensive search for an object within this wide range poses a significant challenge, even for the most efficient object detectors [2]. This challenge becomes particularly pronounced in our specific scenario, where the object detection must identify Rice Leaf Disease (RLD), notably, small objects in vast

open fields. To address this issue with simplicity and specificity, we concentrated our efforts on enhancing the YOLOv7 [3] object detection scale variation.

If scale variation is not properly addressed in RLD detection, it can result in missed detections, false positives, and reduced overall accuracy [4]. For example, if an object detector is designed to only detect objects of a certain size, it may miss smaller or larger objects that are outside of the detector's receptive field. Alternatively, if the detector is designed to detect objects of different sizes, it may be less accurate in detecting objects of a specific shape. By enhancing scale variation in objects of RLD detection, we aim to improve the accuracy and robustness of object detection algorithms, enabling us to accurately detect and classify objects of different sizes and shapes within the image. This can have significant practical applications, such as in agricultural disease monitoring, remote sensing, surveillance, and disaster response, where accurate object detection is critical for decision-making and response planning.

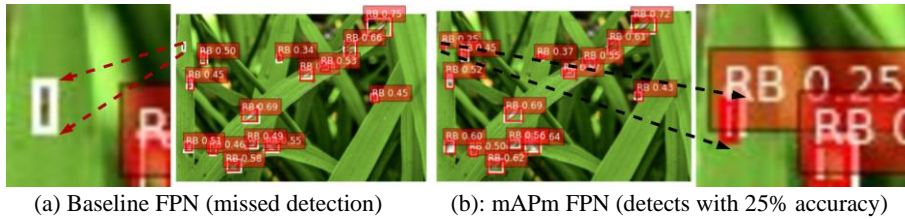


**Fig. 1.** Shows the challenges faced with the baseline FPN due to variations in object characteristics, leading to missed detections, as depicted in (a). In contrast, our approach enhances scaling variation, achieving a 25% average precision in detection, as demonstrated in (b). In the figures, white anchors represent ground-truth annotations, while red anchors indicate the prediction bounding boxes.

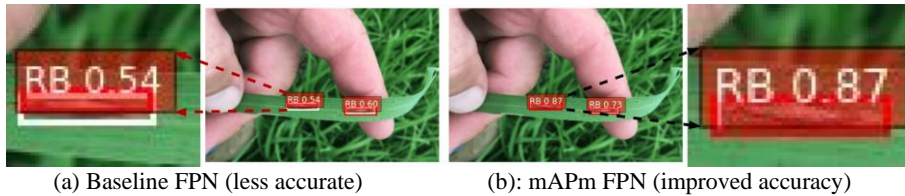


**Fig. 2** shows decreased accuracy with Baseline FPN, as depicted in (a). Then, our approach enhances scale variation, leading to improved accuracy as depicted in (b). Note, the white anchors represent ground-truth annotations, while red anchors indicate the predicted b-boxes.

Previous FPN modules have been proposed to deal with the challenges of scale variation from the earlier times of object detection, one approach is to use an image pyramid [5] at various scales to detect objects but it is memory and computationally expensive because of the large number of images. Another approach is the use of a feature pyramid [6] which in practice is not effective for accurate detection as a result of feature maps closer to the image having a low-level structure. A more advanced approach is the use of a Feature Pyramid Network (FPN) [7] which was introduced in YOLOv3 to improve scale variation, this method works as a feature extractor capable of generating multi-scale feature maps, and then up-scales and combines the information with a corresponding feature level to form the output feature maps. This repeated process of

combining location and rich semantic information from shallow and deep layers significantly improves the performances of YOLOv3 [8], Faster R-CNN [9] and SSD [10] at a certain scale but performs poorly at extremely smaller or larger scales. This is because the working mechanism of FPN does not efficiently use its feature maps to predict appropriate object sizes. This led to further enhanced designs such as PANET [11], Neural Architecture Search Feature Pyramid Network (NAS-FPN) [12], Bi-directional Feature Pyramid Network (BiFPN) [13], and ASPP [14]. While these previous designs have been developed for general applications, our approach is uniquely crafted to address the problem of scale variation in RLD detection. The design of multi-scale Attention Pyramid module (mAPm) is essential because it enable us to harness the full potential of FPN in solving a problem that remains particularly challenging.

mAPm enhances feature maps extraction by replacing conventional convolutions with dilated convolutions at various ratios within the lateral connections of FPN top-down pathways. This modification effectively captures features at various scales. Also, we have refined the up-sampling process through the integration of two key components: a *global* MHSA [15] mechanism and a deconvolutional layer. While the MHSA mechanism enhances network performance by focusing on important features while downplaying less significant ones [15], the deconvolutional layer works to increase spatial resolution, thus preserving fine-grained information.

This study introduces mAPm, a novel self-attention FPN module aimed at enhancing scale-variation in RLD detection, primarily utilized within the YOLOv7 [3] architecture, although adaptable to other frameworks such as Faster R-CNN [9], SSD [10], and RetinaNet [16]. By integrating self-attention mechanisms and atrous convolution, this module effectively captures global context, addressing the challenge of detecting objects at diverse scales encountered in RLD scenarios. Through qualitative and quantitative evaluations, our proposed module demonstrates significant improvements in handling scale variation when compared to state-of-the-art FPN modules.

The contributions of this paper are summarized as follows:

- We propose a novel FPN design called mAPm that utilizes a self-attention mechanism to enhance the preservation of semantic information during the up-sampling of feature maps in the top-down pathway.
- We skillfully integrate atrous convolutions into the lateral connections, enabling the capture of features at multiple scales using dilation ratios. This approach facilitates the simultaneous capture of fine-grained details in a larger context, making the mAPm module effective for addressing scale variations.
- mAPm significantly enhances the detection performance of object detection models when tested with RLD datasets. The results demonstrate a significant improvement in performance after qualitative and quantitative evaluation.
- mAPm modules are versatile and can be integrated into various object detection architectures that use FPN without major architectural changes. This compatibility can enable researchers or developers to enhance existing models easily.

## 2 Related Work

In this section, we explore the evolution and recent advancements in multi-scale variation techniques for object detection. We review various approaches that have evolved over time, each offering distinct advantages and applications while adapting to the dynamic landscape of computer vision.

**Single Layer Methods.** These methods involve handling scale variation independently at all levels where predictions are made in object detection. In this section, we provide an overview of these methods.

*Featurized Image Pyramid (FIP)*, was widely used in the era of hand-engineered features for object detection across multiple scales [7]. It constructs a hierarchical image representation, with each pyramid level representing the image at a different scale. Features are extracted from each level using algorithms like Scale Invariant Feature Transform (SIFT) [17] or Histogram of Oriented Gradient (HOG) [18] and used to train scale-specific object detectors. This approach enables the detector to search for objects at various scales and orientations, enhancing accuracy but less robust, computationally inefficient and slow. While it has been largely replaced by data-driven techniques with the rise of deep learning, it remains relevant in specific scenarios.

*Single Feature Map (SFP)* [5] method, an extension of the FIP approach, is designed to detect objects at multiple scales using a single feature map. It achieves this by employing convolutional filters and pooling operations to progressively reduce the feature map's resolution. Subsequently, specialized object detectors, tailored for different scales, operate on this map to identify objects across varying sizes. SFP is recognized for its simplicity and efficiency, necessitating fewer computational resources compared to the FIP method. This efficiency stems from its operation on a single feature map, facilitating seamless integration with deep learning architectures. However, SFP demands careful tuning of filters and pooling operations to ensure appropriate resolution and receptive fields. This requirement makes it less suitable for highly variable scale scenarios, such as large open farms, where objects of diverse sizes are prevalent.

Another approach, the *Pyramidal Feature Hierarchy (PFH)* method [6] addresses scale variation through a hierarchical neural network architecture. PFH learns features hierarchically, with higher-level features derived from lower-level ones. It consists of multiple layers, each responsible for extracting features at different levels of abstraction. At the lowest level, a Convolutional Neural Network (CNN) processes the input image, extracting low-level features such as edges and corners. These features then pass through pooling layers that progressively reduce resolution and increase the network's receptive field. This hierarchical process continues at higher levels, enabling the learning of features invariant to scale, rotation, and translation. PFH is trained end-to-end using objectives such as cross-entropy loss and has demonstrated superior performance

in various computer vision tasks. Additionally, extensions and variants like Spatial Pyramid Pooling (SPP) [19] and FPN have further expanded its capabilities.

**Multiple Layer Method.** Notably, these methods combine multiple detection layers to improve scale variation in object detection. By merging low-resolution features with higher-resolution maps, it creates a feature pyramid containing valuable semantic content at all levels. This method efficiently constructs image pyramids without much sacrificing information, processing speed, or memory usage.

*Feature Pyramid Network (FPN).* In order to enhance scale-variation, Lin et al. [7] proposes the FPN multi-layer approach for multi-scale object detection, demonstrating its effectiveness in handling scale variation and enhancing detection accuracy. Recent advancements in multiple layers FPN design have introduced several innovative approaches to enhance scale variation and improve object detection accuracy. Tan et al. introduced the BiFPN [13], which efficiently addresses computational costs and enhances the fusion of multi-scale feature maps in EfficientDet architecture, achieving a balance between accuracy and computational efficiency [20]. Meanwhile, the NAS-FPN [12], developed through automated architectural search techniques, presents a novel feature pyramid structure that improves performance, albeit with increased memory requirements [21]. PANet, particularly in the context of instance segmentation, is recognized for its bottom-up pathway augmentation within FPN, enhancing the flow of low-level information to high-level stages and leading to more precise object localization [22].

The recent emergence of self-attention has motivated researchers to explore this mechanism for improving scale-variation due to its strength in capturing long-range and global context. This has led to some work. Hu et al. [23] propose A2-FPN, an Attention Aggregation based Feature Pyramid Network for instance segmentation. By addressing limitations in traditional FPNs, A2-FPN improves multi-scale feature learning through attention-guided aggregation techniques. Their method consistently enhances performance across various frameworks, yielding significant improvements in mask AP when integrated into Mask R-CNN and other strong baseline models. Cao et al. [24] introduce ACFPN, an Attention-guided Context Feature Pyramid Network for object detection. It addresses the challenge of balancing feature map resolution and receptive field on high-resolution inputs by integrating attention-guided multi-path features. ACFPN consists of two modules: Context Extraction Module (CEM) and Attention-guided Module (AM), which significantly improve object detection and instance segmentation performance.

While there has been some work integrating self-attention mechanisms to improve FPNs, the exploration has been limited. We aim to explore attention mechanisms for enhancing scale-variation in FPNs by demonstrating their potential when integrated with dilated convolutions. Specifically, we will enhance scale variation in YOLOv7 for RLD detection.

### 3 Method and Tools

#### 3.1 YOLOv7

YOLO is a typical one-stage object detection method i.e., it simultaneously performs both localization and classification, unlike two-stage methods that use RPN (Region Proposal Network) which significantly increase computational cost. This unique design choice makes YOLO faster in training and inference time, thus, well-suited for real-time object detection tasks. In real-time detection, YOLO detects target objects of various scales in three levels using the FPN, having each level performs localization and classification with location and semantic information respectively. We employed YOLOv7 [3] which utilizes CSPDarknet-53 [3] as it's backbone network, featuring 52 convolutions and skip-connections. This backbone network is responsible for extracting features from the input image. Subsequently, the model learns to generate predicted bounding boxes based on the extracted features. Finally, Non-Maximum Suppression (NMS) is applied to produce the final results, Fig. 3.

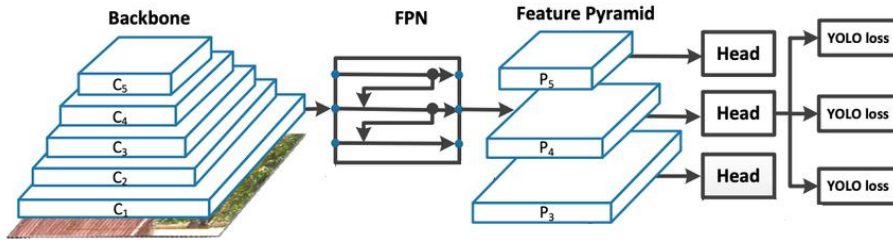


Fig. 3. YOLOv7 network architecture

To recap, YOLO excels in real-time detection and is easily adaptable for scale variation thanks to its efficient handling of various object sizes in a single pass, making it well-suited for real-time applications like in RLD detection tasks. The use of anchor boxes and its ability to integrate enhancements like FPN further enhance its performance in handling scale variation while maintaining speed.

#### 3.2 mAPm Architectural Design

Motivated by the recent success of attention mechanism in CV, we proposed mAPm, a novel attention module designed to enhance scale-variation in RLD detection. It achieves this by leveraging a combination of attention mechanism and atrous convolution. The module integrates a *global* MHSA component to improve information loss caused by up-sampling in the FPN top-down pathway. By incorporating global attention, the module ensures that important contextual information is preserved across different scales. Then, we replaced the notable  $3 \times 3$  convolutional layer in the FPN lateral connections with parallel atrous convolutions of scale  $\{1, 2, 3\}$ . This modification allows the module to capture various scales of objects by expanding the receptive fields without significantly increasing computational overhead. Overall, these design choices enhance the inherent scale variation in detecting RLD within the YOLOv7 framework, leading to improved accuracy and robustness in object detection tasks.

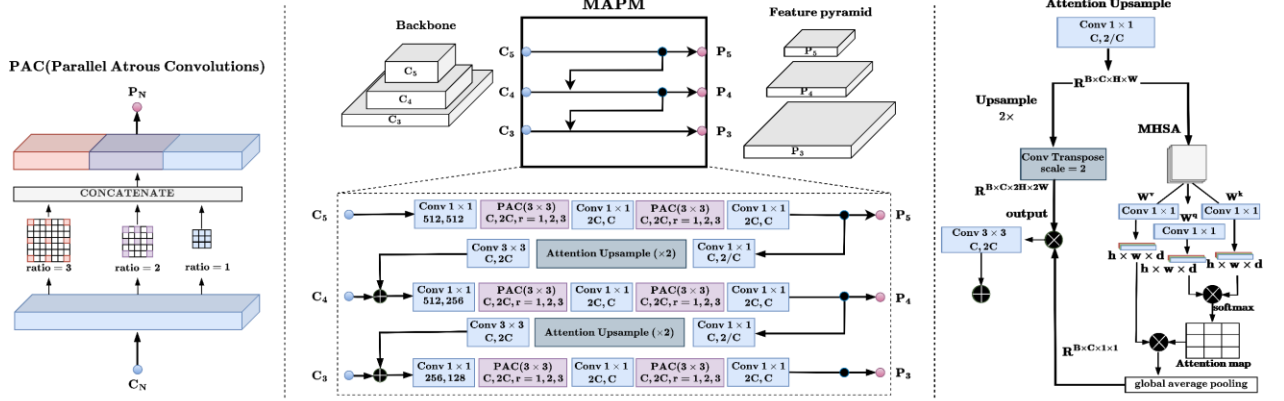


Fig. 4. mAPm architecture in YOLOv7

### 3.3 mAPm Architectural Components

**Lateral Connection:** RLD images are inherently complex, featuring objects of interest that exhibit a wide range of scale variations, from extremely small to large. This presents a significant challenge for most general-purpose object detection systems, often leading to false positive detections and miss detection. Such inaccuracies can have devastating consequences, particularly in fields like plant disease detection, where the accurate detection of objects is of utmost importance. Therefore, we intend to improve the capture capability of semantic information on the lateral connections.

The YOLOv7 FPN incorporates three lateral connections  $C_3, C_4,$  and  $C_5$  to process feature maps from the bottom-up pathway, progressively reducing spatial scale dimensions while enhancing semantic richness. Within each lateral connection, there are two blocks, each originally consisting of a  $(\text{Conv } 3 \times 3, C, 2C)$  layer followed by a  $(\text{Conv } 1 \times 1, 2C, C)$  layer, similar to depth-wise convolutions.

To improve capturing objects at varying scales, we expand the receptive field through dilated convolution. The receptive field refers to the area of the input image that a particular neuron in the network can "see" or take into account when making predictions. The receptive field is calculated in equation 1.

$$R_n^{(i)} = R_{n-1}^{(i)} + (K - 1) \times d_i \quad (1)$$

Where,  $i = 1, 2, 3$  is the scale factors

$R_n$  is the receptive field at layer

$R_{n-1}$  is the receptive field at the previous layer

$K$  is the kernel size (filter size).

$d_i$  is the dilation rate.

Increasing  $d_i$  expands  $R_n^{(i)}$  of each neuron in the network, enabling it to capture information from a larger area of the input image. This facilitates the detection of objects at varying scales by allowing the network to consider details from a broader context. This redesign offers enhanced capabilities for capturing scale variations in complex

plant imagery like RLD by facilitating multi-scale feature extraction, preserving fine details, and adapting efficiently to variable plant structures, which distinguishes it from normal convolutions.

In our modification, we replaced the  $3 \times 3$  convolutional layer in the FPN lateral connections with parallel atrous convolutions (PAC) featuring  $\{1, 2, 3\}$  scale ratios in parallel (Fig. 4), we aim to preserve information at various scales. Let  $F_n^{(i)}$  represent the feature map obtained from the  $i^{th}$  scale factor atrous convolution at layer  $n$ . The concatenation of these feature maps obtained from different dilation rates is then represented in equation 2.

$$\text{PAC} = \text{concat}(F_n^{(1)}, F_n^{(2)}, F_n^{(3)}) \quad (2)$$

**Attention Up-sampled:** In the vanilla FPN design, feature maps from different layers of the backbone network are utilized to propagate semantic information. While lower layers of deep neural network typically capture low-level features, the higher layers capture more abstract, semantic information about the content of the image. To leverage these disparities in value between the low and higher layers, FPN fuses the two layers together, technically passing the information from lower layers to higher layers. This fusion enhances object localization and understanding, as the network can use both fine-grained and high-level information at each layer. Before fusion, up-sampling of higher-level features becomes necessary due to the unequal spatial resolutions between the low and high levels, resulting in information loss. To enhance this limitation, we integrated a global MHSA into the up-sampling operation to mitigate the loss of information.

For mAPm, we created a dual path for the input tensor in the top-down pathway. The tensor has a shape of  $X \in \mathbb{R}^{B \times C \times H \times W}$  as input for the 2D global MHSA operation. Then, we process the input into MHSA in three steps:

- *Projection:* We first project the input feature map  $X$  into query, key, and value matrices using learnable linear projections

$$Q = XW_q, K = XW_k, \text{ and } V = XW_v$$

Where,  $W_q, W_k,$  and  $W_v$  are learnable weight matrices used for projection

- *Scaled Dot-Product Attention:* Next, we compute the attention scores  $A$  between all pairs of positions in the input feature map, as in equation 3.

$$A = \text{softmax} \left( \frac{QK^T}{\sqrt{d_k}} \right) \quad (3)$$

Where  $d_k$  is the dimension of the key vectors.

- *Weighted sum:* We then compute the output feature map  $Y$  as a weighted sum of the value vector  $V$ , weighted by the attention scores  $A$ , equation 4.

$$Y = AV \quad (4)$$

Subsequently, we apply global average pooling to the MHSA output, resulting in a shape of  $Y \in \mathbb{R}^{B \times C \times 1 \times 1}$ . We then perform element-wise multiplication between  $Y$  and the resulting deconvolutionally up-sampled feature map, denoted as up-sample =  $\mathbb{R}^{B \times C \times 2H \times 2W}$  (Fig. 4). This approach enhances the up-sampling operation of the FPN, enabling it to simultaneously consider fine-grained details and broader context. This



modification effectively minimizes information loss during the up-sampling operation within the top-down pathway of the FPN. Note that while nearest-neighbor and bilinear interpolations are alternative options, deconvolution has proven to be more effective for up-sampling due to its learnable nature and adaptability to specific tasks. This design choice minimizes information loss during up-sampling, thereby significantly enhancing the top-down pathway of the FPN.

## 4 Experiment

In this section, we evaluate the mAPm module on MRLD [25] dataset both qualitatively and quantitatively. We then assess its generalization using the COCO [26] dataset. Our approach is compared with other state-of-the-art models to validate its effectiveness in improving scale variation in RLD.

**Dataset and metric.** We conduct experiments on the MRLD, which contains 5,932 images of four disease categories: Blast, Bacterial blight, Tungro, and Brown Spot. Then, we utilize the COCO dataset, which comprises 330,000 images across 80 object classes. We use the Average Precision (AP) and mean Average Precision (mAP) to evaluate the performance of our model. AP and mAP are formulated as shown in equations (5) and (6).

$$AP = \frac{1}{11} + \sum_{Recall \in \{0,0.1,\dots,1\}} Precision(Recall_i) = 1 \quad (5)$$

$$mAP = \frac{1}{N} \sum_{i=1}^N AP_i \quad (6)$$

**Experimental setup.** We initialized the default YOLOv7 network settings, and the CSPDarknet-53 network as backbone. The bias values for the classification and localization layers in the detection head were set to 0.01 and 0.1, respectively. A Gaussian weight with  $\sigma = 0.01$  was used in all layers, including the proposed feature selection network. We employed the AdamW optimizer with an initial learning rate of 0.001, weight decay of 0.0009, and momentum of 0.9. Our implementation was carried out on a Linux-based system with an Intel Core i7 8700k processor, 2 NVIDIA Titan XP 12GB GPUs, and 32GB of RAM. For fairness, we trained the comparative models in the same environment and from scratch.

### 4.1 Qualitative Evaluation with Bounding Boxes and mAP scores.

We examined the bounding boxes and the mAP scores of four RL diseases, namely, BB, BS, RB, and TG. Subsequently, we conducted a comparative analysis of mAPm performance against several state-of-the-art scale variation modules, namely baseline FPN [7], BiFPN [13], NAS-FPN [12], PANET [22], and ACFPN [24]. Our findings

reveal a significant enhancement in mAP scores for detecting disease objects in rice leaves using the mAPm module Fig. 1. This improvement can be attributed to the enhanced design of the MAPM module by integrating *global* MHSA mechanism and dilated convolutions, which effectively addresses scale variation challenges.

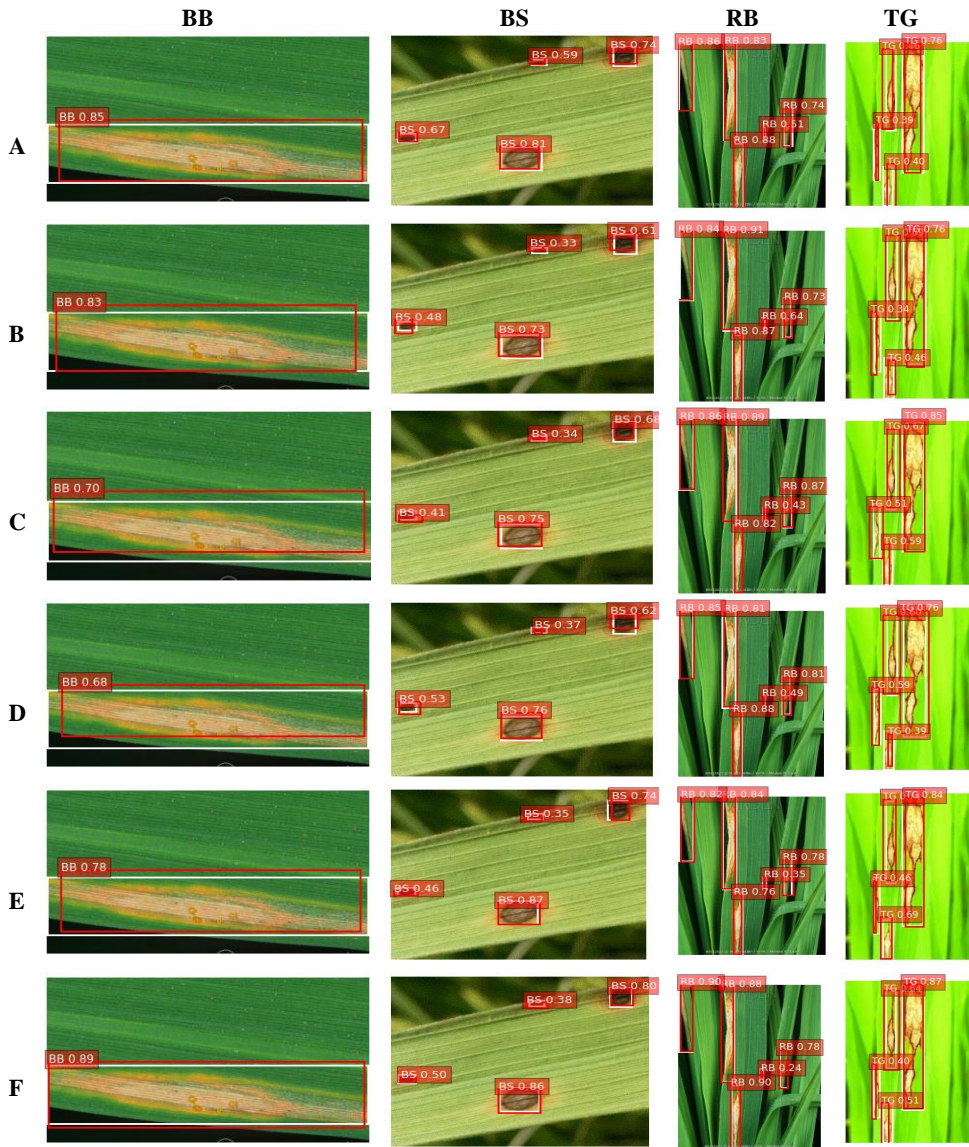


**Fig. 5.** Bounding boxes visualization and mAP comparison with FPN (A), BiFPN (B), NAS-FPN (C), PANET (D), ACFPN (E), and mAPm (F). The white b-box is the ground-truth while the red color is the predicted b-box.

**Bounding Boxes on Tiny objects variation:** In this section, our focus is on smaller objects or those with varying characteristics. Through visualizations, we highlight the challenges posed by tiny object variations, such as reduced accuracy and the likelihood of missing objects, emphasizing the necessity for precise detection methods. We comprehensively compare mAPm to several state-of-the-art scale variation modules, including the baseline FPN [7], BiFPN [13], NAS-FPN [12], PANET [22], and ACFPN [24]. The visualizations offer insights into the precision and effectiveness of bounding box detection, particularly for objects with small size variations. Our findings reveal a notable improvement in mAP scores when detecting these challenging objects, underscoring the significance of mAPm modules in effectively addressing the nuances of tiny object variations.

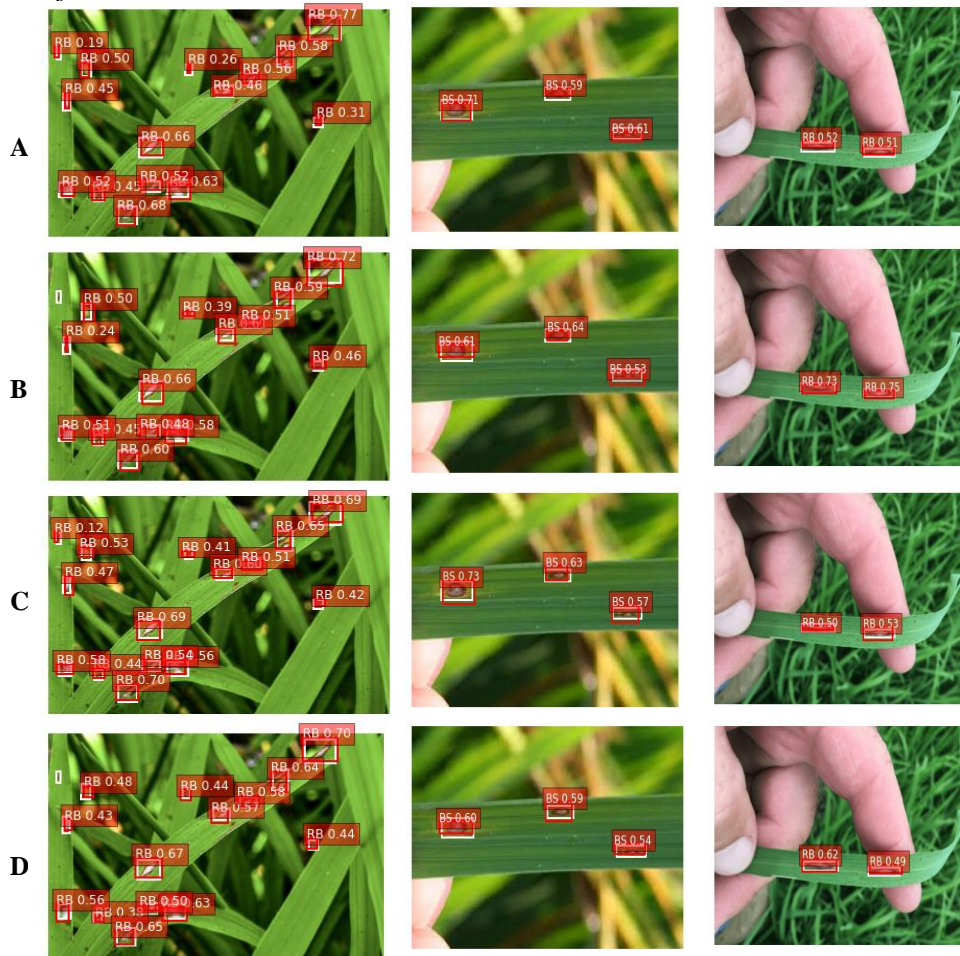
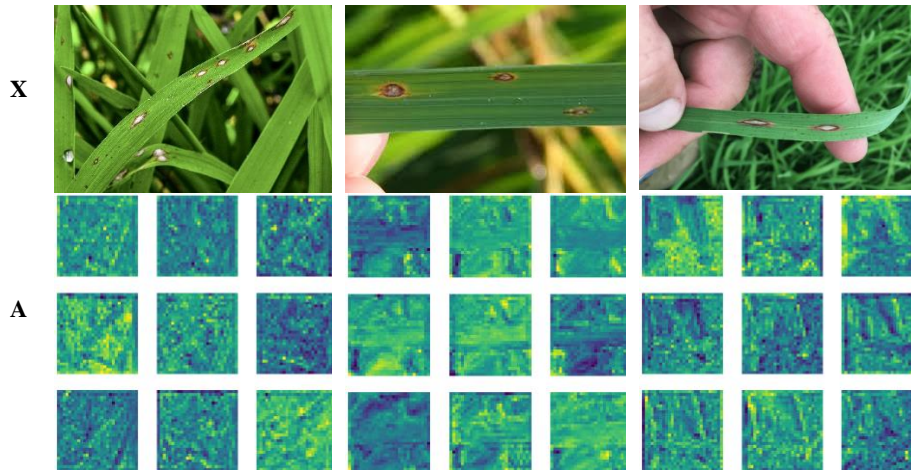






**Fig. 6** Bounding boxes visualization and mAP comparison on tiny objects with FPN (A), BiFPN (B), NAS-FPN (C), PANET (D), ACFPN (E), and mAPm (F).

**Feature map visualization on the last layer (P5) of MAPM.** We conducted a feature map visualization of the last layer (P5) within the mAPm module to gain insights into how this module mitigates spatial information loss. We compared these results with those obtained from several state-of-the-art scale variation network modules, namely baseline FPN [7], BiFPN [13], NAS-FPN [12], PANET [22], and ACFPN [24]. Our analysis revealed a significant enhancement in the preservation of spatial information and the capture of global information within the mAPm modules, (Fig. 7). This improvement can be attributed to the integration of dilated convolutions and global MHSA mechanisms in the lateral connections and top-down pathway, respectively. As a result, the network’s capability to detect objects of various scales, including small objects commonly found in RLD images, has been substantially improved.



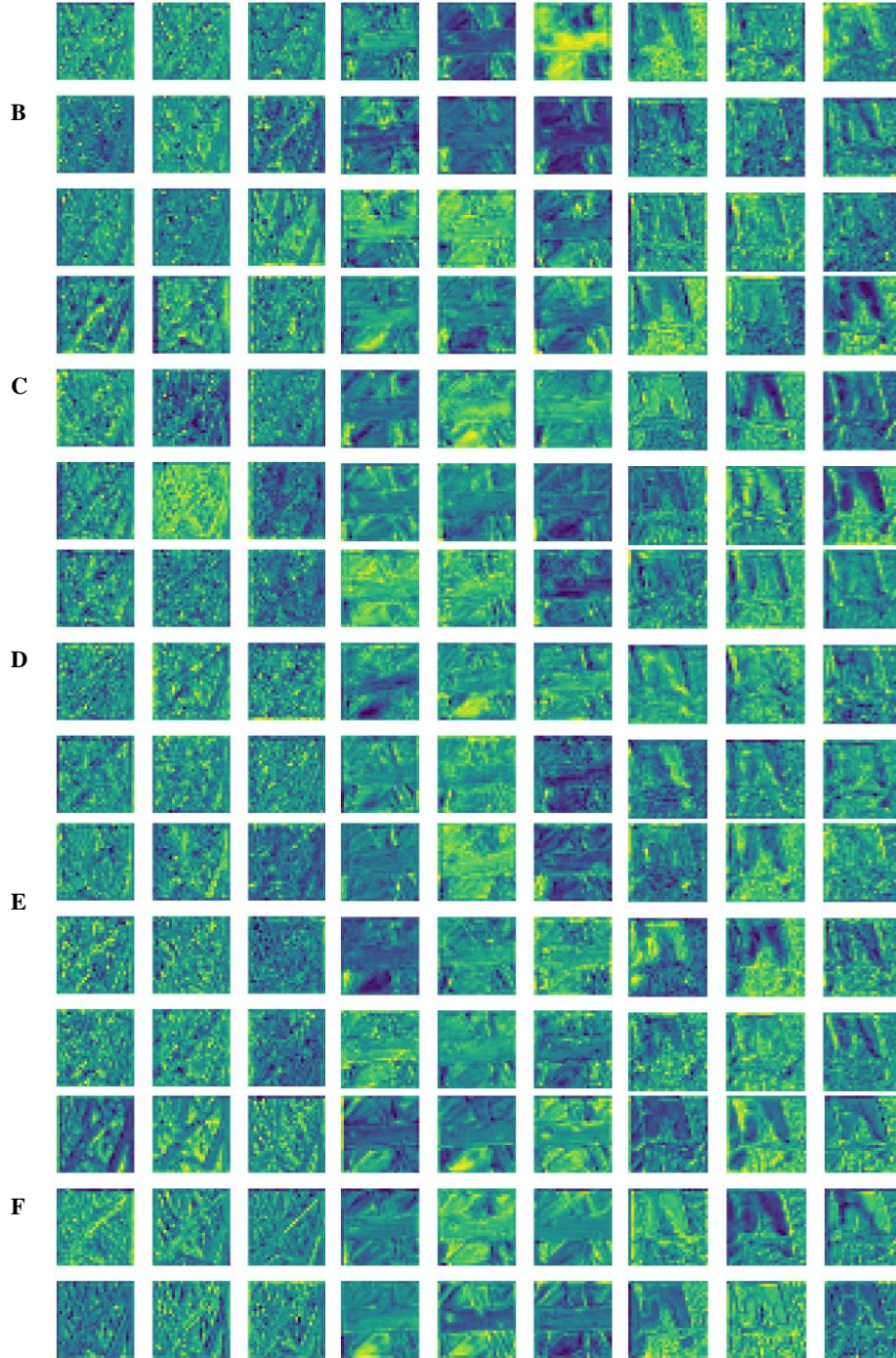


**Fig. 7** Feature map comparison of mAPm module with baseline FPN (A), BiFPN (B), NAS-FPN (C), PANET (D), ACFPN (E), and mAPm (F). X is the input image.

## 4.2 Quantitative Evaluation of mAPm and Comparisons.

We conducted  $AP$  metrics on various state-of-the-art feature pyramid modules and compared the results with our approach. Table 1 demonstrates an improvement in scale variation compared to other methods for detecting RLD. For example, we observed a +2.91% increase in  $AP$  compared to the FPN (baseline) and a +3.10% increase for  $AP_S$ . Our approach consistently outperforms other feature pyramid methods across a range of OD models, particularly excelling in detecting small and medium-sized objects. These findings indicate the effectiveness of mAPm in enhancing scale variation in object detection.

**Table 1** Object detection methods comparison with different FPN design (*mini-val*)

Feature Pyramid	Methods	$AP$	$AP_{50}$	$AP_{75}$	$AP_S$	$AP_M$	$AP_L$
BiFPN	F. R-CNN	40.95	61.71	46.89	23.76	46.36	52.57
	RetinaNet	40.89	59.33	47.18	23.21	43.48	49.79
	SSD	39.18	58.61	44.95	23.27	43.45	49.35
	YOLOv7	38.18	58.14	41.29	22.86	42.87	47.36
NAS-FPN	F. R-CNN	39.38	59.68	44.56	22.82	43.54	50.82
	RetinaNet	38.34	58.76	41.43	22.25	42.87	50.19
	SSD	37.46	58.58	41.2	22.12	41.76	47.64
	YOLOv7	36.73	57.47	39.78	21.57	41.5	46.64
PANET	F. R-CNN	39.15	59.95	46.22	22.52	45.39	50.51
	RetinaNet	38.78	59.28	44.58	22.16	45.0	49.41
	SSD	38.58	58.21	41.85	22.15	44.9	48.39
	YOLOv7	36.84	57.82	40.9	20.48	42.86	46.72
ACFPN	F. R-CNN	38.75	57.84	43.26	22.19	42.72	50.2
	RetinaNet	37.49	57.41	42.93	21.77	42.19	48.93
	SSD	35.55	57.79	40.85	20.3	41.29	48.55
	YOLOv7	35.67	55.73	39.36	19.63	40.09	46.0
FPN	F. R-CNN	38.6	59.11	45.72	23.14	45.64	52.16
	RetinaNet	37.01	58.74	45.08	22.83	44.32	51.08
	SSD	37.18	58.38	43.07	22.12	42.85	49.7
	YOLOv7	36.92	56.87	41.12	21.53	42.72	49.33
mAPm (Ours)	F. R-CNN	41.51	63.21	49.66	26.24	46.28	53.63
	RetinaNet	41.37	60.37	48.52	25.33	46.21	53.25
	SSD	40.44	57.73	48.15	23.79	43.93	52.62
	YOLOv7	40.35	57.51	46.49	23.4	43.82	50.02

**Comparison with (test-dev) datasets:** In table 2, we conducted a similar experiment on the *test-dev* dataset to further evaluate our approach. The results show a significant improvement compared to other methods. Specifically, we achieved a +2.61% increase in  $AP$  with the baseline FPN in YOLOv7 when compared to our approach, and a +0.37% increment in  $AP_L$  compared to the FPN baseline in YOLOv7.

**Table 2** Object detection methods comparison with different FPN design (*test-dev*)

Feature Pyramid	Methods	AP	AP <sub>50</sub>	AP <sub>75</sub>	AP <sub>S</sub>	AP <sub>M</sub>	AP <sub>L</sub>
BiFPN	F. R-CNN	39.87	60.82	46.49	23.28	45.92	51.89
	RetinaNet	39.71	58.94	46.28	22.98	43.11	49.51
	SSD	38.51	58.15	44.21	22.95	43.06	49.14
	YOLOv7	36.78	57.79	40.35	22.43	42.5	46.92
NAS-FPN	F. R-CNN	38.73	59.26	43.64	22.33	43.07	50.58
	RetinaNet	37.15	58.48	40.92	21.97	42.58	49.82
	SSD	36.78	57.84	40.69	21.77	41.5	46.93
	YOLOv7	36.4	57.01	39.08	21.16	41.18	46.3
PANET	F. R-CNN	38.71	59.45	45.67	22.12	44.92	50.31
	RetinaNet	37.92	58.52	44.34	21.73	44.74	49.02
	SSD	37.85	58.0	41.44	21.72	44.55	47.58
	YOLOv7	36.05	57.54	40.45	20.0	42.41	46.24
ACFPN	F. R-CNN	37.79	57.38	42.43	21.78	42.34	49.46
	RetinaNet	37.23	57.08	42.41	21.28	41.86	48.51
	SSD	34.82	56.9	40.18	20.03	41.02	48.1
	YOLOv7	34.3	55.43	38.91	19.36	39.73	45.52
FPN	F. R-CNN	37.28	58.72	44.82	22.7	45.36	51.91
	RetinaNet	36.75	57.84	44.42	22.43	44.11	50.74
	SSD	36.63	57.65	42.74	21.84	42.59	49.47
	YOLOv7	36.36	56.64	40.64	21.09	42.23	48.84
mAPm (Ours)	F. R-CNN	40.59	62.59	49.21	25.92	46.05	53.05
	RetinaNet	40.2	59.96	48.08	24.84	45.78	52.78
	SSD	39.02	57.11	47.94	23.43	43.7	52.42
	YOLOv7	38.97	57.01	46.16	23.1	43.4	49.21

**mAP comparison across various categories:** We conducted another evaluation based on the categories of RLD using mAP metrics and added more models for comparison. We integrated mAPm with Faster R-CNN, and the results in Table 3 show that our method improves the mAP scores by +3.8% compared to the Faster R-CNN baseline (FPN). These results highlight the effectiveness of integrating MHSA and dilated convolution into the FPN to improve scale variation in object detection models, emphasizing its potential for accurate and reliable disease detection.

**Table 3** mAP performance comparison with state-of-the-art object detection models

Method	F. R-CNN	L. R-CNN	SSD	YOLOv7	DETR	RetinaNet	Ours
BB	74.40	47.33	40.04	52.27	61.21	45.06	72.80
BS	66.69	64.94	59.49	51.08	65.53	47.78	69.96
RB	64.59	63.04	51.15	46.85	66.46	52.52	61.75
TG	57.76	54.76	42.71	55.01	57.16	51.25	74.11
mAP	65.86	57.52	48.35	51.30	62.59	49.15	69.66

**Evaluation on COCO dataset.** To determine the generalization of our approach, Table 4 provides a comprehensive performance comparison of object detection methods across two categories: Two-stage methods and Single-stage methods. The evaluation is based on the widely used COCO dataset, with metrics include AP, AP at IoU thresholds of 0.50 ( $AP_{50}$ ) and 0.75 ( $AP_{75}$ ), as well as class-specific APs for small ( $AP_S$ ), medium ( $AP_M$ ), and large ( $AP_L$ ) objects. These results collectively offer valuable insights into the performance of a range of object detection methods. Furthermore, we conducted extensive testing of the mAPm on various state-of-the-art OD models. The findings from these evaluations reveal a notable and consistent improvement in the detection module's performance. This outcome not only highlights the effectiveness of the mAPm module in addressing the specific challenges posed by RLD images but also suggests its potential as a robust and reliable solution for broader image analysis tasks.

**Table 4** Object Detection results (Bounding Box AP) on COCO (minival). Note

<b>Methods (2-stage)</b>	<b>Backbone</b>	<b>AP</b>	<b><math>AP_{50}</math></b>	<b><math>AP_{75}</math></b>	<b><math>AP_S</math></b>	<b><math>AP_M</math></b>	<b><math>AP_L</math></b>
Cascade R-CNN	Restnet-101	39.22	59.8	44.07	22.85	44.82	50.76
DETR	Restnet-50	38.71	57.38	43.5	22.24	43.07	49.74
Faster R-CNN	Restnet-101	37.58	56.29	43.2	22.01	42.40	49.67
Faster R-CNN	ResNeXt-101(64-4d)	36.68	56.24	42.05	21.98	42.08	49.58
Libra R-CNN	Restnet-101	36.28	56.19	41.81	21.66	41.74	49.03
TridentNet	Restnet-101	36.02	55.42	41.23	21.00	40.53	48.60
Cascade R-CNN (■)	Restnet-101	39.47	60.13	44.52	23.34	45.41	51.19
DETR (■)	Restnet-50	38.83	57.79	43.72	22.42	43.49	49.89
F. R-CNN (■)	Restnet-101	37.83	56.61	43.6	22.50	42.71	50.24
F. R-CNN (■)	ResNeXt-101(64-4d)	36.96	56.53	42.51	22.44	42.65	49.98
L. R-CNN (■)	Restnet-101	36.56	56.57	42.12	21.89	41.94	49.44
TridentNet (■)	Restnet-101	36.12	55.68	41.51	21.26	41.01	49.32
<b>Methods (1-stage)</b>							
RetinaNet	Restnet-101	37.76	58.45	43.25	21.53	44.28	50.24
RetinaNet	ResNeXt-101(64-4d)	37.95	56.1	42.23	21.12	42.5	48.95
SSD	Restnet-101	36.18	54.88	41.73	20.57	41.4	48.59
YOLOv3	CSBDarknet-53	35.91	55.69	41.16	20.66	40.61	48.21
YOLOv5	Restnet-101	35.27	54.87	41.0	20.93	41.14	48.33
YOLOv7	Restnet-101	35.1	54.28	40.44	20.45	39.59	47.66
RetinaNet (■)	Restnet-101	38.26	59.42	44.64	22.69	45.38	50.86
RetinaNet (■)	ResNeXt-101(64-4d)	38.73	56.24	42.44	22.01	44.05	49.79
SSD (■)	Restnet-101	36.44	55.74	42.16	21.62	42.47	49.85
YOLOv3 (■)	CSBDarknet-53	36.2	56.18	42.6	21.18	41.48	48.49
YOLOv5 (■)	Restnet-101	36.32	55.53	41.94	22.26	41.48	48.67
YOLOv7 (■)	Restnet-101	35.35	55.34	40.78	20.95	41.19	48.38

Note (■) denotes mAPm was used instead of the baseline FPN.



## 5 Conclusion

In conclusion, our research enhances the challenge of scale variation in object detection, specifically in RLD images. While OD has achieved success in computer vision, varying object scales remain a significant obstacle, leading to missed detections and reduced accuracy. To tackle this, we propose the Multi-scale Attention Pyramid Module (mAPm) within the YOLOv7 architecture. mAPm integrates dilated convolutions in lateral connections for effective feature extraction across scales and enhances up-sampling with a global Multi-Head Self-Attention (MHSA) mechanism and learnable deconvolutional layers. Our experiments demonstrate substantial improvements, particularly in RLD datasets, highlighting mAPm effectiveness. Its compatibility with existing OD architectures underscores its practicality, offering a valuable tool for accurate and robust object detection across scales in diverse domains such as agriculture, surveillance, and disaster response.

**Funding statement.** No funding was received for conducting this study.

**Financial declaration.** The authors have no relevant financial or non-financial interest to disclose.

**Disclosure of Interests.** The authors have no competing interests to declare that are relevant to the content of this article.

## References

1. Ding, Jian, Nan Xue, Yang Long, Gui-Song Xia, and Qikai Lu. Learning roi transformer for oriented object detection in aerial images [A]. In Proceedings of the IEEE/CVF Conference on Computer Vision and Pattern Recognition [C], pp. 2849-2858. 2019.
2. Liu, Li, Wanli Ouyang, Xiaogang Wang, Paul Fieguth, Jie Chen, Xinwang Liu, and Matti Pietikäinen. Deep learning for generic object detection: A survey [J]. *International journal of computer vision* 128 (2020): 261-318.
3. Wang, Chien-Yao, Alexey Bochkovskiy, and Hong-Yuan Mark Liao. "YOLOv7: Trainable bag-of-freebies sets new state-of-the-art for real-time object detectors." In Proceedings of the IEEE/CVF Conference on Computer Vision and Pattern Recognition, pp. 7464-7475. 2023.
4. Kellenberger, Benjamin, Diego Marcos, and Devis Tuia. Detecting mammals in UAV images: Best practices to address a substantially imbalanced dataset with deep learning [J]. *Remote sensing of environment* 216 (2018): 139-153.
5. Kim, Seung-Wook, Hyong-Keun Kook, Jee-Young Sun, Mun-Cheon Kang, and Sung-Jea Ko. Parallel feature pyramid network for object detection [A]. In Proceedings of the European conference on computer vision (ECCV) [C], pp. 234-250. 2018.
6. Farabet, Clement, Camille Couprie, Laurent Najman, and Yann LeCun. Learning hierarchical features for scene labeling [J]. *IEEE transactions on pattern analysis and machine intelligence* 35, no. 8 (2012): 1915-1929.

7. Lin, T.Y., Dollár, P., Girshick, R., He, K., Hariharan, B., Belongie, S.: Feature pyramid networks for object detection [A]. In: Proceedings of the IEEE conference on computer vision and pattern recognition [C]. pp. 2117–2125 (2017)
8. Redmon, Joseph, and Ali Farhadi. "Yolov3: An incremental improvement." arXiv preprint arXiv:1804.02767 (2018).
9. Ren, Shaoqing, Kaiming He, Ross Girshick, and Jian Sun. "Faster r-cnn: Towards real-time object detection with region proposal networks." *Advances in neural information processing systems* 28 (2015).
10. Liu, Wei, Dragomir Anguelov, Dumitru Erhan, Christian Szegedy, Scott Reed, Cheng-Yang Fu, and Alexander C. Berg. "Ssd: Single shot multibox detector." In *Computer Vision–ECCV 2016: 14th European Conference, Amsterdam, The Netherlands, October 11–14, 2016, Proceedings, Part I* 14, pp. 21–37. Springer International Publishing, 2016.
11. Liu, Shu, Lu Qi, Haifang Qin, Jianping Shi, and Jiaya Jia. "Path aggregation network for instance segmentation." In *Proceedings of the IEEE conference on computer vision and pattern recognition*, pp. 8759–8768. 2018.
12. Ghiasi, Golnaz, Tsung-Yi Lin, and Quoc V. Le. "Nas-fpn: Learning scalable feature pyramid architecture for object detection." In *Proceedings of the IEEE/CVF conference on computer vision and pattern recognition*, pp. 7036–7045. 2019.
13. Tan, Mingxing, Ruoming Pang, and Quoc V. Le. "Efficientdet: Scalable and efficient object detection." In *Proceedings of the IEEE/CVF conference on computer vision and pattern recognition*, pp. 10781–10790. 2020.
14. Chen, Liang-Chieh, George Papandreou, Iasonas Kokkinos, Kevin Murphy, and Alan L. Yuille. "DeepLab: Semantic image segmentation with deep convolutional nets, atrous convolution, and fully connected crfs." *IEEE transactions on pattern analysis and machine intelligence* 40, no. 4 (2017): 834–848.
15. Srinivas, Aravind, Tsung-Yi Lin, Niki Parmar, Jonathon Shlens, Pieter Abbeel, and Ashish Vaswani. "Bottleneck transformers for visual recognition." In *Proceedings of the IEEE/CVF conference on computer vision and pattern recognition*, pp. 16519–16529. 2021.
16. Lin, Tsung-Yi, Priya Goyal, Ross Girshick, Kaiming He, and Piotr Dollár. "Focal loss for dense object detection." In *Proceedings of the IEEE international conference on computer vision*, pp. 2980–2988. 2017.
17. Lindeberg, Tony. "Scale invariant feature transform." (2012): 10491.
18. Dalal, Navneet, and Bill Triggs. "Histograms of oriented gradients for human detection." In *2005 IEEE computer society conference on computer vision and pattern recognition (CVPR'05)*, vol. 1, pp. 886–893. Ieee, 2005.
19. He, Kaiming, Xiangyu Zhang, Shaoqing Ren, and Jian Sun. "Spatial pyramid pooling in deep convolutional networks for visual recognition." *IEEE transactions on pattern analysis and machine intelligence* 37, no. 9 (2015): 1904–1916.
20. Pallathadka, Harikumar, Pavankumar Ravipati, Guna Sekhar Sajja, Khongdet Phasinam, Thanwamas Kassanuk, Domenic T. Sanchez, and P. Prabhu. Application of machine learning techniques in rice leaf disease detection [J]. *Materials Today: Proceedings* 51 (2022): 2277–2280.
21. Girshick, Ross, Jeff Donahue, Trevor Darrell, and Jitendra Malik. Rich feature hierarchies for accurate object detection and semantic segmentation [A]. In *Proceedings of the IEEE conference on computer vision and pattern recognition [C]*, pp. 580–587. 2014.
22. Ott, Patrick, and Mark Everingham. Shared parts for deformable part-based models [A]. In *CVPR 2011 [C]*, pp. 1513–1520. IEEE, 2011.

23. Zhu, Yingying, Jiong Wang, Lingxi Xie, and Liang Zheng. "Attention-based pyramid aggregation network for visual place recognition." In Proceedings of the 26th ACM international conference on Multimedia, pp. 99-107. 2018.
24. Cao, Junxu, Qi Chen, Jun Guo, and Ruichao Shi. "Attention-guided context feature pyramid network for object detection." arXiv preprint arXiv:2005.11475 (2020).
25. Sethy, Prabira Kumar, Nalini Kanta Barpanda, Amiya Kumar Rath, and Santi Kumari Behera. "Deep feature based rice leaf disease identification using support vector machine." *Computers and Electronics in Agriculture* 175 (2020): 105527.
26. Lin, Tsung-Yi, Michael Maire, Serge Belongie, James Hays, Pietro Perona, Deva Ramanan, Piotr Dollár, and C. Lawrence Zitnick. "Microsoft coco: Common objects in context." In *Computer Vision—ECCV 2014: 13th European Conference, Zurich, Switzerland, September 6-12, 2014, Proceedings, Part V* 13, pp. 740-755. Springer International Publishing, 2014.